

## Proton Damage Effects on P-Channel CCDs

G R Hopkinson, *Member, IEEE*

Sira Electro-Optics Ltd, South Hill, Chislehurst, Kent BR7 5EH, UK

### Abstract

An experimental batch of p-buried channel CCDs has been fabricated and characterised for proton-induced radiation damage. Dark current effects were similar to conventional n-channel CCDs, but radiation-induced changes in charge transfer inefficiency were reduced by approximately a factor 3 for  $-30^{\circ}\text{C}$  operation and background signal  $\sim 2,000$  electrons/pixel; though this is a lower limit and further reduction may be possible in future CCD batches.

### I. INTRODUCTION

Though CMOS active pixel sensors [1-3] offer great promise for use in spaceborne imaging instruments, most applications still rely on charge-coupled device (CCD) technology to provide low noise sensors with a uniform response and wide dynamic range. However, it is well known that CCDs are particularly vulnerable to displacement damage effects on both dark current and charge transfer inefficiency, CTI, (see for example [4, 5]).

For low Earth applications these effects can usually be accommodated by cooling the CCD. This reduces dark current and increases the emission time constants of trapping states in the buried channel (so that once filled, the traps do not interact over the timescales of interest). Use of a background charge (or 'fat zero') can also give a dramatic improvement in CTI (by as much as a factor 10 [6]) and a notched (or supplementary) buried channel can be useful in small-signal applications in confining the charge into a smaller volume. However, new classes of applications are emerging where the environment is harsher and possibilities for device cooling are reduced. For example, star trackers and ISL (inter satellite link) terminals in geostationary, intermediate and high low-earth orbits.

For these applications it would be greatly advantageous if the radiation tolerance of CCDs could be improved. It has recently been suggested by Spratt et al [7] that using boron rather than phosphorous as the buried channel dopant will reduce the concentration of phosphorous-vacancy complexes (E-centers) in the buried channel and thus remove the primary radiation-induced defect responsible for charge transfer degradation. The idea of using p-buried channel devices is not new. For example Saks et al [8] studied total dose effects in p-channel CCDs with a dual oxide/nitride dielectric, but they concentrated solely on total dose effects. Displacement damage effects are of more fundamental importance for the space environment since ways of hardening the dielectric are well known (for example Holmes-Seidle et al [9] discuss the use of dual oxide/nitride dielectric with n-channel CCDs).

The previous p-channel work [7] indicated that dark current and CTI effects were indeed reduced; however, the dependence of CTI on signal size and background was not characterised nor were dark current measurements reported in detail. This study makes an in-depth attempt to relate the CTI and dark current behaviour of p- and n-channel devices of similar architecture and to investigate any side-effects or drawbacks to the use of p-channel technology.

A preliminary feasibility study, undertaken by the CCD manufacturer (EEV Ltd, Chelmsford, UK), indicated that it should be possible to adapt their process to p-channel without the need for changes in the mask set or fabrication equipment. This assumption was proved correct since acceptable image quality devices were produced at the first attempt. This is an important finding in its own right since it demonstrates that p-channel device fabrication is essentially straightforward in principle.

It was found that clock voltages have to be carefully optimized to avoid spurious clock-induced dark signal. This is because electrons are present at the surface of a p-channel device in partially inverted mode (rather than holes at the surface of an n-channel CCD). The impact ionization rate is significantly higher for electrons.

Total dose effects were similar to those for n-channel devices and so too was the radiation-induced bulk dark current. This is not too surprising since the technology for forming the gate dielectric is similar in both cases (though the electric field across the dielectric will be in the opposite sense), and the phosphorous present in the n-type substrate will lead to the formation of E-centers throughout most of the depletion region (though very few in the p-type buried channel itself). In the same way as for n-channel CCDs, the most troublesome dark current defects are produced in high field regions of the depletion region and their generation rate is increased due to field-enhanced emission. Random telegraph behaviour was also observed in a similar way to n-channel CCDs [10]. The charge transfer efficiency was, however, seen to be improved in p-channel devices (by approximately a factor 3), and the emission time of the traps in the p-type silicon is reduced. Unfortunately, due to a processing anomaly during manufacture (possible over-etching due to a power failure), we cannot rule out the possibility that the radiation-induced CTI is linked to an observed high pre-irradiation CTI and is caused by total dose rather than bulk trapping effects. Hence we can only establish an upper limit to the CTI. Fabrication of a second batch of devices will be needed to decide if further improvements are possible.

### A. Nomenclature, Units and Proton Test Energy

Since the carriers in a p-channel CCD are holes, parameters such as signal size should be expressed in numbers of holes rather than electrons. However, to avoid confusion when making comparison with n-channel devices, we will continue to express signals in electrons.

The main concern of this paper is the charge transfer degradation, due to displacement damage. This is usually assumed to be proportional the non-ionizing energy loss (NIEL) for any particular proton energy so that the total 'displacement damage dose' is the integral of the product of the differential proton spectrum and the non-ionizing energy loss at each proton energy. This can be expressed either in units of MeV/g or as an equivalent number of protons at a convenient test energy (e.g. 10 MeV): see, for example [4] and the references therein for a more detailed discussion. As an example of a relevant environment, 10 years in a 1400 km orbit behind 10mm aluminum shielding will give a displacement damage dose of  $\sim 10^9$  MeV/g or an equivalent fluence of  $\sim 10^{11}$  10 MeV protons/cm<sup>2</sup>. Such an environment would give a total ionizing dose of around 70 krad (Si).

The advantage of the NIEL concept is that testing is only needed at a single proton energy, In this case 10 MeV. In future studies it would be useful to perform testing at other (in particular, higher) proton energies in order to check the proportionality between CTI and NIEL. An approximate check was, however, performed using 5.48 MeV alpha as described below.

At 10 MeV, a total dose of 1 krad (Si) is deposited by a fluence of  $1.8 \times 10^9$  protons/cm<sup>2</sup>. Hence the fluence in p/cm<sup>2</sup> can be converted to a total ionizing dose and vice versa. Since some effects (e.g. dark current increase) can be due to both total ionizing dose and displacement damage effects, it is useful to be aware of both quantities. In the following, the data plots are usually labelled with total dose in krad(Si) but the conversion to proton fluence is straightforward using the above conversion factor.

## II. EXPERIMENTAL DETAILS

The devices were a p-channel version of the standard EEV 3 phase CCD02, which has 288x385 (22  $\mu$ m x 22  $\mu$ m) image area pixels. They were non-inverted mode operation (non-IMO, or non-multi-phase-pinned) but were operated in a partially inverted mode (two of the three phases inverted). Some IMO devices were fabricated but their horizontal CTI was poor, possibly because of the inclusion of an IMO barrier in the serial register, which reduces the maximum transfer rate (this IMO barrier was a by-product of the use the existing mask set and would not normally be present). The devices were all fabricated on n/n<sup>+</sup> [111] silicon using, almost entirely, the standard EEV n-channel process but with boron buried channel and source/drain implants.

Test equipment, details of the irradiation facility and the spot illumination technique for CTI measurement were as given

previously [6]. In addition, an improved technique, known as the first pixel response (FPR), was used for measuring vertical CTI. This was first discussed by Gregory et al [11]. In a frame transfer CCD the basic principal is to use flat field illumination to provide signal charge and to use the split in the electrode structure between the image and storage region clocks to move the storage region charge towards the readout register and hence to create a 'gap' in the flat field image (equivalently the image region clocks can be operated backwards so as to move charge away from the image/storage boundary). The creation of the gap gives a sharp edge to the signal region (Figure 1), the first line of which loses charge due to trapping. Subsequent lines experience less charge loss because the traps are partially filled (by the signal in preceding lines). Eventually (after several lines into the signal region) an equilibrium is reached where charge loss equals charge deferred. The CTI can then be calculated from the difference ( $\Delta S$ ) between this equilibrium signal value ( $S$ ) and the first line of signal pixels (the first pixel response):

$$CTI = 1 - [1 - (\Delta S/S)]^{1/N} \quad (1)$$

where N is the number of line transfers needed for readout.

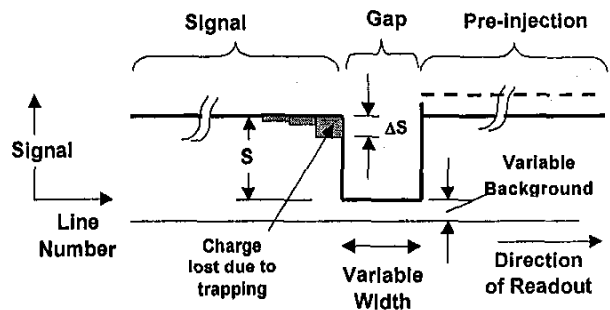


Figure 1 Vertical slice (column direction) through a CCD image showing signal versus line number when using a clocking sequence for First Pixel Response (FPR) measurements.

With this clocking technique there is inevitably charge (from the illumination) present in the lines before and after the 'gap'. This is so that the gap can be created electronically (by clocking) rather than optically (e.g. by imaging of a knife edge), which is less sharp. The charge readout in front of the 'gap' acts to fill traps ahead of the charge after the gap and so acts as a pre-injection charge pulse. The width of the 'gap' can be varied so that the emission times of traps can be measured (if the time to clock charge through the gap region is much longer than the emission time then the traps have time to empty and a 'worst-case' CTI is measured). If the 'gap' region (together with the 'signal' region) is momentarily exposed to illumination (before readout) then a variable background signal can be created; likewise the charge in the 'signal' and 'pre-injection' regions can be independently varied (by exposure to illumination for controlled periods). To shield pixels from illumination during readout a store shield can be positioned over the storage region, alternatively, a mechanical shutter or LED

pulse illumination can be used. For full-frame devices the gap can be formed at the boundary between the area clock electrodes and the readout register – though in this case there is no possibility for pre-injection. For devices with a split readout register (not applicable in this particular case), the technique can be used to determine horizontal CTI.

The FPR technique therefore allows full control of clock timing as well as signal, background and pre-injection levels. It has been used both with n- and p-channel CCDs. However, in the present (p-channel) study the presence of a large pre-irradiation CTI (with its own dependence on signal and background levels) caused complications, with the result that there was more scatter in the CTI data than in previous n-channel investigations.

Emission times were measured using the FPR technique, as discussed above and also using spot illumination. With spot illumination the most straightforward measurement is to make an exposure of the spot image, frame transfer the image to the storage region and then to perform additional transfers by repeatedly moving the image *one* pixel vertically and then one pixel back again, with a variable delay between transfers. If this delay ( $\Delta T$ ) is short then filled traps do not have time to emit their charge before the signal packet is transferred back into the pixel and the CTI is reduced according to:

$$CTI = CTI_0 [1 - \exp(-\Delta T/\tau_e)] \quad (2)$$

Where  $CTI_0$  is the 'worst case' CTI which is measured at long delay times. With the FPR method,  $\Delta T$  in equation (2) is the time taken to clock pixels through the 'gap' region shown in Figure 1. With both techniques it was checked that variations in CTI were not due to capture time effects. The capture time was estimated by measuring CTI as a function of dwell time within a pixel and found by to be significantly  $< 1 \mu s$  for the signal sizes of interest here. Hence the capture time did not have an effect on the measurements of emission time.

The voltages applied to the CCDs are based on those for n-channel devices except that the polarity is reversed with respect to the substrate voltage. However it was necessary to fine-tune the clock voltages in order to avoid spurious charge otherwise the field at the edge of the CCD column isolation can be high enough for impact ionization to occur. The effect is important for p-channel devices since at typical field strengths ( $10^5$  V/cm) the impact ionization rate is an order of magnitude higher for electrons than holes [12]. The spurious charge is not dependent on integration time and does not change with temperature in the same way as thermal dark charge. The spurious charge does however vary due to changes in the impact ionization rate, which increases as the temperature decreases (At room temperature the effect was much less significant than at  $-30^\circ C$ .) Some n-channel CCDs also show the effect when operated in inverted mode (but usually to a much lesser extent). With these n-channel CCDs the spurious charge can be ameliorated by slowing the clock waveforms and/or tri-level clocking [13].

Figure 2 shows the effect on dark charge at  $-30^\circ C$ , of varying the clock high voltage (equivalent to the clock low voltage on an n-channel CCD). There is a pronounced drop in dark signal as the clock voltage is reduced. Note that the spurious charge was spatially non-uniform, hence the plots for the 0, 10 and 30 krad(Si) regions of the image, for any given CCD, do not decrease at the same rate. By reducing the clock high voltage the spurious charge could be made negligible and it will not be discussed further in this paper.

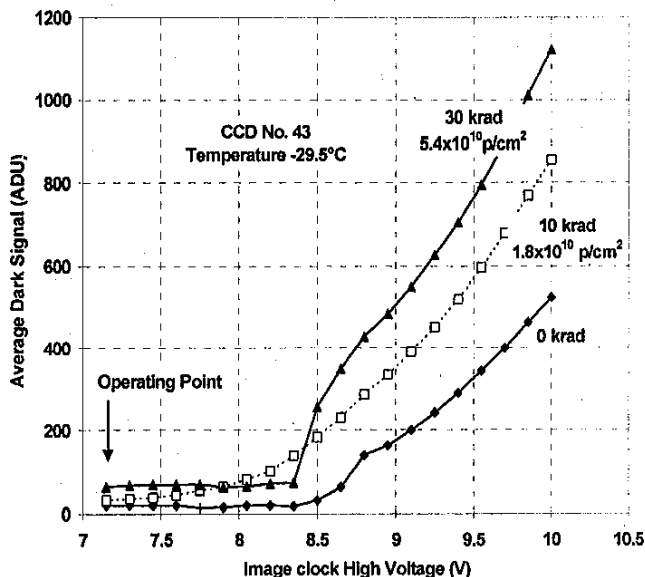


Figure 2 Average dark signal versus clock high voltage (equivalent to clock low voltage for an n-channel CCD).

Five devices (both biased and un-biased) were irradiated with 10 MeV protons with various fluences in the range  $3.6 \times 10^9$  to  $5.4 \times 10^{10}$  p/cm<sup>2</sup> at the Tandem Van de Graaff accelerator at AEA Technology, Harwell, UK. Also, two CCDs were given 5.48 MeV alpha irradiation from a 2.59 kBq Am241 source in the laboratory. (One at room temperature, the other at an average of  $\sim -20^\circ C$ .) Annealing measurements were also performed at temperatures up to  $150^\circ C$  as described below. Measurements included charge to voltage conversion factor (CVF, in  $\mu V$ /electron), full well capacity, flatband voltage shift, dark current and charge transfer inefficiency (CTI). Though not accurately measured, the flatband shift was not seen to be significantly different from that seen previously with n-channel devices [4] and the maximum total dose was not enough to cause measurable changes in CVF or full well capacity. The remainder of this paper will concentrate on dark current and CTI effects.

### III. RESULTS

To illustrate the good imaging performance after irradiation, Figure 3 shows an image taken with a typical device (#46) at moderate light levels and also a section of a dark image. However such images are not quantitatively useful since the presence of background charge (from the scene) tends to give an over-optimistic impression of CTI performance (compared with spot or FPR data).

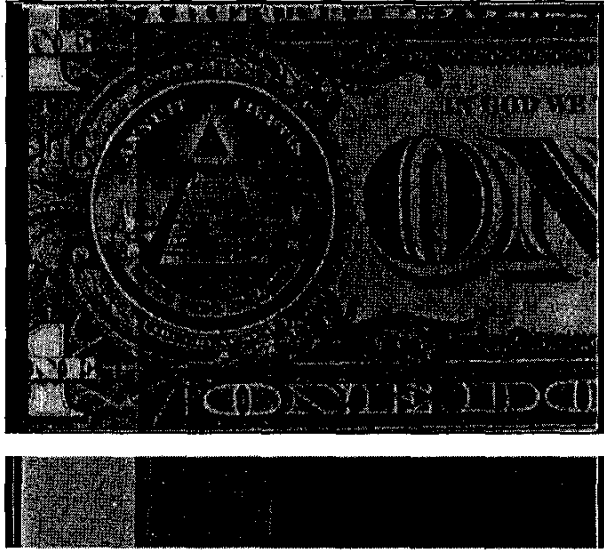


Figure 3 Image obtained at moderate light levels and part of a dark image; the dose regions being, from left to right, 10, 4, 0 and 2 krad(Si) 10 MeV protons (fluences of  $1.8 \times 10^{10}$ ,  $7.2 \times 10^9$ , 0 and  $3.6 \times 10^9$  p/cm<sup>2</sup>).

A. Dark current

Figure 4 shows average image region dark current results for several devices (including an IMO device, designated #42i in the figure). At 25°C the increase after irradiation was ~ 1 nA/cm<sup>2</sup>/krad(Si). This value is due to total dose-induced surface dark current and is very similar to that found for n-channel EEV CCDs [4].

Although the IMO device has a reduced dark current it was not possible to fully invert the surface and the surface dark current was only reduced by a factor ~ 2. This was not unexpected since no attempt was made to optimise the design of the IMO implant.

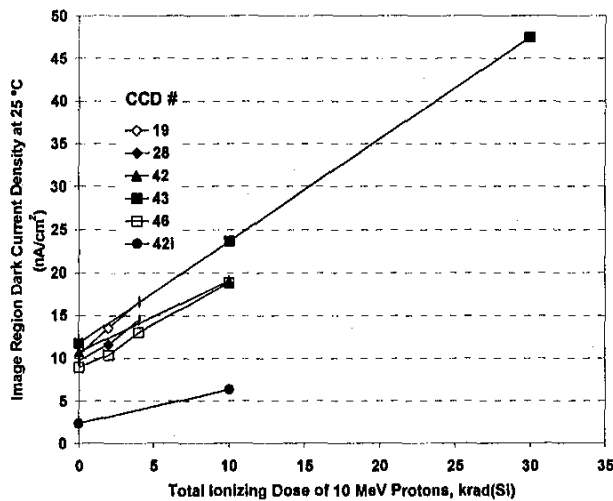


Figure 4 Average image region dark current density. The IMO device data is represented by filled circles (•)

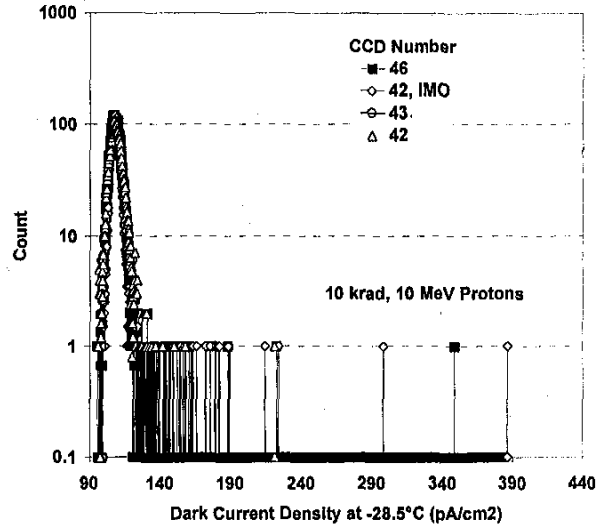


Figure 5 Histograms of dark current density after 10 krad(Si) 10 MeV protons for four devices

Figure 5 gives dark current histograms for four devices after 10 krad(Si) ( $1.8 \times 10^{10}$  p/cm<sup>2</sup>) showing that dark current spikes due to bulk displacement damage are present.

The temperature behavior of the dark current was studied over the range -40°C to +25°C and found to follow the expected relation

$$\text{dark signal} = \text{constant} \exp(-E_{\text{act}}/kT) \quad (3)$$

where  $E_{\text{act}}$  is an activation energy. Figure 6 shows that most pixels have the usual value for silicon (around 0.63 eV) but that the brightest spikes show a reduced activation energy indicative of field enhanced emission [14].

There was no significant dependence on the irradiation bias (in either the mean level or the non-uniformity).

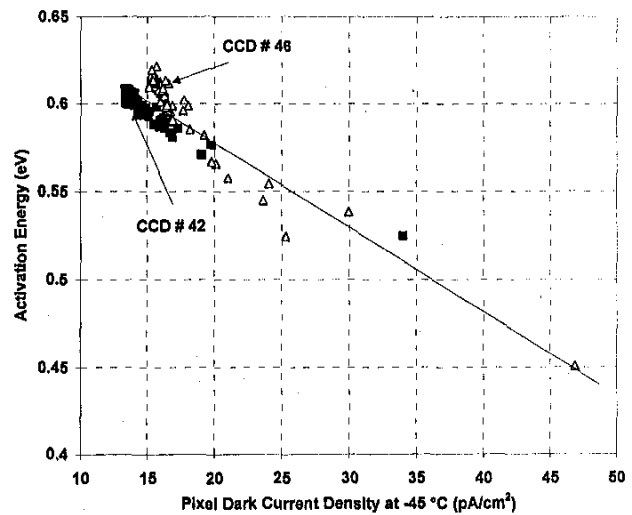


Figure 6 Activation energy for the brightest pixels on two CCDs. The straight line is drawn by eye for indication only.

Alpha particle irradiation ( to a fluence of  $1.7 \times 10^8 / \text{cm}^2$ ) produced similar dark current histograms to Figure 5 (allowing for the factor 60 increase in non-ionizing energy loss for 5.84 MeV alphas compared with 10 MeV protons [15]).

Figure 7 shows random telegraph signals (RTS's) at  $-30^\circ\text{C}$  for 6 of the brightest pixels on two devices. Some pixels (such as A, B and F) show large fluctuations, whilst others (e.g. E) show changes comparable with the readout noise level. The time constants appear to be of the order of one hour. This is considerably shorter than predicted from near-room temperature measurements on n-channel CCDs, but it should be noted that the low temperature behavior of RTS fluctuations is not well understood. (A previous study on n-channel CCDs [16] also showed shorter than expected time constants at low temperatures:  $-20^\circ\text{C}$  in that case.)

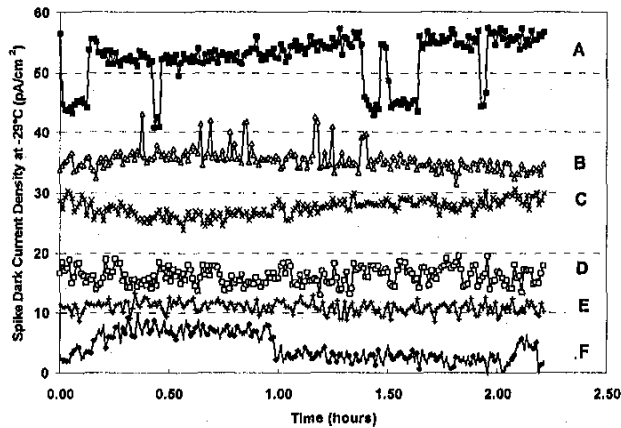


Figure 7 Random telegraph signals from a proton irradiated p-channel CCD at  $-29^\circ\text{C}$ .

After five 1 hour isochronal annealing steps up to  $147^\circ\text{C}$  (61, 81, 102, 123 and  $147^\circ\text{C}$ ) there was some reduction in the brightest dark current spikes but the general conclusion was that, for practical temperatures that could be achieved in flight (i.e.  $<100^\circ\text{C}$ ), annealing of defects is not significant (this applied to CTI data also). Annealing of dark current spikes (assuming they are due to E-centers) can be expected at temperatures above  $150^\circ\text{C}$  but this was not attempted due to the small number of available devices. Divacancies are not expected to anneal until temperatures  $\sim 400^\circ\text{C}$ .

### B. Charge Transfer Inefficiency (CTI)

Both spot illumination and FPR measurements gave similar estimates of the CTI. Figure 8 shows results at  $-30^\circ\text{C}$ , showing that the pre-irradiation CTI is significant for these particular devices. Figure 9 shows the radiation-induced CTI (the pre-irradiation value have been subtracted). Comparing this data with previous Sira measurements on n-channel CCD02 devices (both published [6] and unpublished) indicates a factor  $\sim 3$  improvement for the p-channel CCDs. Care was taken to compare data sets for the same conditions of signal, background and clocking rate. Note: the CTI

versus signal and background plots given in [6] refer to a line move time of  $0.66 \mu\text{s}$ , these values have to be increased by a factor  $\sim 2$  to allow for the slower line move time ( $\sim 300 \mu\text{s}$ ) used in this case. This factor 2 increase can be derived from figure 12 of [6] and has been confirmed by subsequent (unpublished measurements) on EEV n-channel CCDs for a range of signals and backgrounds. Clock overlap times in all these measurements were similar enough not to cause significant errors in the comparisons.

Most measurements were made at a background  $\sim 2,000$  electrons/pixel, however the lower dark current for the IMO device allowed a measurement at  $\sim 450$  electrons/pixel. This gave a similar CTI, whereas for n-channel devices this reduction in background results in a CTI roughly a factor 2 higher (for similar signal levels). Hence it is suspected that the improvement in CTI may be higher (i.e. greater than a factor 3) at lower backgrounds, though further measurements on a new batch (without the high pre-irradiation CTI) will be needed to confirm this.

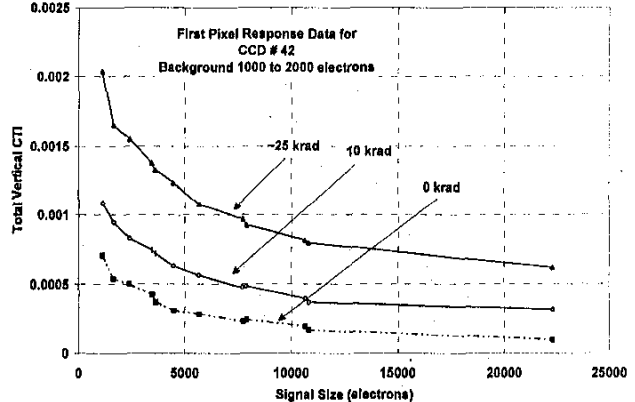


Figure 8 CTI versus signal size for one device. Note the significant pre-irradiation value.

Figure 10 shows data on the emission time obtained four months after irradiation (in this case from spot-illumination measurements). There is a factor 2.25 difference between the emission times at  $-45^\circ\text{C}$  and  $-28^\circ\text{C}$  and this indicates a trap energy of  $\sim 0.25 \text{ eV}$  above the valence band. This is consistent with literature values for the divacancy. The absolute values for  $\tau_e$  should also agree with predictions using

$$\tau_e = \exp(E/kT) / \sigma_p X_p v_{th} N_v \chi \quad (4)$$

where

- $n_p$  = hole density within the buried channel
- $\sigma_p$  = capture cross section for mobile holes
- $v_{th}$  = average thermal velocity for holes
- $N_v$  = effective density of states in the valence band
- $T$  = absolute temperature
- $k$  = Boltzmann's constant
- $X_p$  = the 'entropy factor' associated with the entropy change for hole emission from the trap
- $\chi$  = field enhancement factor
- $E$  = energy level of the trap above the valence band.

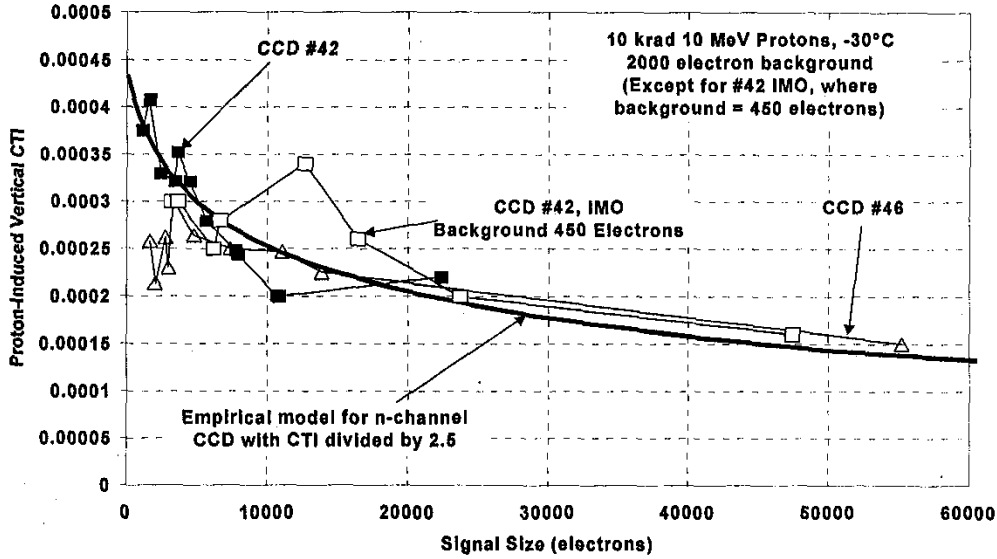


Figure 9 Radiation-induced CTI for three different p-channel CCDs. The pre-irradiation CTI has been subtracted. The scatter in the data is due to experimental errors.

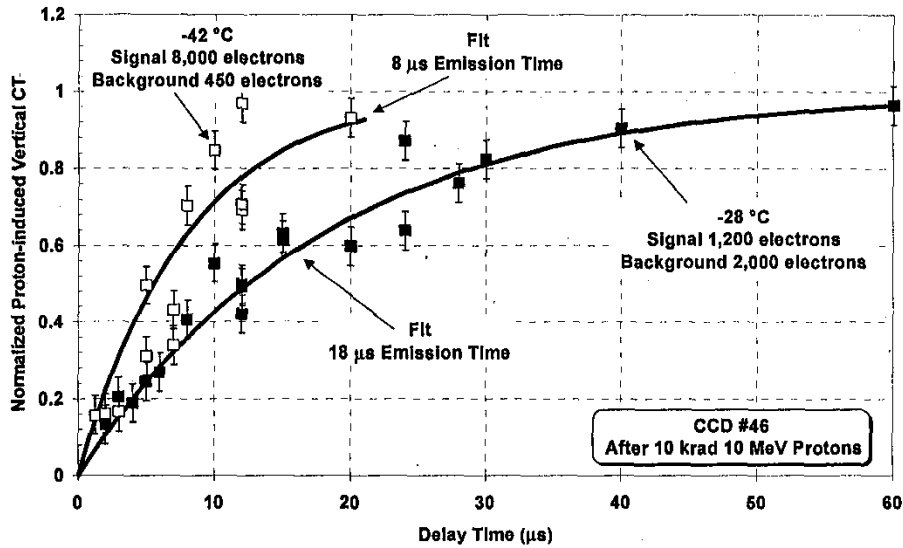


Figure 10 Emission time constant measurements and theoretical fits using equation (2)

Hence to estimate the expected emission time we need the value of  $v_{th}N_c$  for holes (the value for electrons is  $4.11 \times 10^{25} (77/T)^2$  [17]).  $N_v$  and  $v_{th}$  depend on the values of the hole effective masses (the density of states effective mass and the conduction effective mass). Szé [12] gives different values for the density of states for electrons and holes ( $N_c$  and  $N_v$ , respectively):

$$N_c = 2(2\pi (M_c^{2/3} m_{dc})kT/h^2)^{3/2} \quad (5)$$

$$N_v = 2(2\pi m_{dh}kT/h^2)^{3/2} \quad (6)$$

$$v_{th} = (3kT/m^*)^{1/2} \quad (7)$$

where  $m_{dc}$  and  $m_{dh}$  are the density of states effective masses for electrons and holes and  $M_c$  is the number of equivalent

energy states for electrons (= 6, for silicon). Size gives the values of  $N_c$  and  $N_v$  as  $2.8 \times 10^{19} \text{ cm}^{-3}$  and  $1.04 \times 10^{19} \text{ cm}^{-3}$  respectively, however more recent work by Vankemmel et al [18] gives a higher hole effective mass, such that  $m_{dh}$  and  $(M_c^{2/3} m_{dc})$  are similar. This implies that  $N_c$  and  $N_v$  should be similar also. For electrons, the effective mass for conduction ( $m^*$ ) is close to  $m_{dh}$  and the value for holes should be approximately a factor  $M_c^{2/3}$  ( $= 6^{2/3} = 3.3$ ) larger. Hence  $v_{th}$  should be a factor  $6^{2/3}$  smaller. We end up with a value of  $v_{th}N_v$  for holes a factor  $6^{2/3}$  smaller than  $v_{th}N_c$  for electrons. This gives agreement with the observed emission time provided  $\sigma_p X_p \chi \sim 10^{-16} \text{ cm}^2$ . A value which still gives acceptable values for the capture time:

$$\tau_c = 1/\sigma_p v_{th} n_s \quad (8)$$

The measurements also agreed with values obtained from the alpha irradiated devices.

Note however that this cannot be considered as definitive evidence that the radiation-induced CTI is caused by divacancies. CTI data obtained soon after irradiation showed fluctuating values for the emission time constant (tending to be slightly higher). The situation is complicated by the high pre-irradiation CTI and the chance that the processing anomaly during manufacture rendered the CTI sensitive to total dose effects (which may change with time due to build up of interface traps). All that can be said with certainty is that the emission time is considerably shorter than the value for the E-center (~ 1 ms at -30°C) which is found in n-buried channel devices. Additional annealing experiments and more detailed temperature characterisation of the emission time may be feasible with future CCD batches and would help to determine the nature of the hole trap responsible for CTI degradation with more confidence.

#### IV SUMMARY

It is important for the emerging communication satellite market that imaging sensors are developed which can withstand proton environments giving total doses behind shielding in the range 10-100 krad. The principal technologies available are the CMOS active pixel sensor and the CCD. Of the two, the CCD is the more mature technology but proton-induced CTE degradation is a major drawback. Work at Sira and elsewhere is ongoing in the areas of APS (active pixel sensor) testing and improving n-channel CTE performance by choice of pixel architecture and provision of background charge.

This programme has demonstrated the feasibility of an alternative approach. P-channel devices require some care in the avoidance of clock-induced change (particularly at low temperatures) but otherwise appear straightforward to fabricate. It is to be expected that the high pre-irradiation CTI can be eliminated in any future batch and the improvement in radiation-induced CTI should be at least a factor 3, probably more for the low background case.

#### ACKNOWLEDGEMENTS

Peter Jameson, the Study Manager at the Defence Evaluation and Research Agency (DERA), Farnborough, UK, is thanked for his help and support. The efforts of EEV Ltd (in particular Peter Pool, Kevin Ball and David Burt) are greatly appreciated.

#### REFERENCES

- [1] O. Yadid-Pecht, C. Clark, B. Pain, C. Staller, and E. R. Fossum, "Wide dynamic range APS star tracker" *Proc SPIE*, 2654, 82-92, 1996.
- [2] G. Meynants, B. Dierickx and D. Scheffer, "CMOS Active Pixel sensor with CCD performance", *Proc SPIE*, vol. 3410, pp 68-76, 1998.
- [3] O. Saint-Pe, R. Davencens, M. Tulet, P. Magnan, C. Cavadore, A. Gautrand, Y. Degerli, F. Lavernhe and J. Farre, "Development and Characterisation of Active Pixel Sensors for Space Applications, *Proc SPIE*, vol. 3440, pp24-36, 1998.
- [4] G. R. Hopkinson, C. J Dale, and P. W. Marshall, 'Proton effects in CCDs', *IEEE Trans. on Nuclear Science*, vol. NS-43(2), pp 614-627, 1996.
- [5] T. Hardy, R. Murowinski and M. J. Deen, "Charge Transfer Efficiency in Proton damaged CCD's", *IEEE Trans. on Nuclear Science* vol. NS-45(2), pp. 154-163, 1998.
- [6] I. H Hopkins, G. R. Hopkinson and B. Johlander, 'Proton-Induced Charge Transfer Degradation in CCDs for Near-Room Temperature Applications', *IEEE Trans. on Nuclear Science* vol. NS-41(6), pp. 1984-1990, 1994.
- [7] J. P. Spratt, B. C. Passenheim and R. E. Leadon, "The Effects of Nuclear Radiation on P-channel CCD Imagers", *IEEE Radiation effects data Workshop*, pp116-121, 1997.
- [8] N. S. Saks, J. M. Killiany, P. R Reid and W. D. Baker, 'A radiation hard MNOS CCD for low temperature applications', *IEEE Trans. on Nuclear Science* vol. NS-26(6), pp. 5074-5079, 1979.
- [9] A. Holmes-Seidle, K. Egan and S. Watts, 'Trapped Charge in Dual-dielectric CCDs and MOSFETs' 1999 *IEEE Nuclear and Space Radiation Effects Conference*.
- [10] G. R. Hopkinson 'Proton Irradiation Induced RTS in CCDs' Proc 14th Int. Conf. on 'Noise in Physical Systems and 1/f Fluctuations', Ed. C. Claeys and E. Simoen, pp 218-223, World Scientific, Singapore 1997.
- [11] J. A. Gregory, B. E. Burke and M. J. Cooper, *Solid State Research, Quarterly Technical report (ESC-TR-92-149)*, Lincoln laboratory, MIT, 31 Jan 1993, pp 48-50).
- [12] S. M. Sze, 'Physics of Semiconductor Devices', 2<sup>nd</sup> Edn, p 47, Wiley-Interscience, 1981.
- [13] J. Janesick, "CCD transfer method - standard for absolute performance of CCDs and digital camera systems", *Proc SPIE*, vol. 3019, pp 70-102, 1997.
- [14] J. R. Srour and R. A. Hartmann, 'Enhanced displacement damage effectiveness in irradiated silicon devices', *IEEE Trans. on Nuclear Science*, vol. 36, pp. 1825-1830, 1989.
- [15] C. J. Dale, P. W. Marshall, B. Cummings, L. Shamey and A. Delamere, "Spacecraft displacement Damage Dose calculations for Shielded CCDs", *Proc SPIE*, vol. 1656, pp 476-487, 1992.
- [16] I. H. Hopkins and G. R. Hopkinson, "Further Measurements of Random Telegraph Signals in Proton Irradiated CCDs", *IEEE Trans. on Nuclear Science*, vol. 42, pp. 2074-2081, 1995.
- [17] E. K. Banghart, J. P. Lavine, E. A. Trabka, E. T. Nelson and B. C. Burkey, 'A Model for Charge Transfer in Buried Channel Charge-Coupled Devices at Low Temperatures', *IEEE Trans. on Electron Devices*, vol. 38(3), pp 1162-1174, 1991.
- [18] R. Vankemmel, W. Schoenmaker and K. de Meyer, "A Unified Wide Temperature Range Model for the Energy Gap, the Effective Carrier Mass and Intrinsic Concentration in Silicon", *Solid-state Electronics*, Vol. 36(10), pp 1379-1384, 1993.